POLITECNICO DI TORINO
Repository ISTITUZIONALE

Detailed versus aggregated modeling in energy community operation optimization

Original
Detailed versus aggregated modeling in energy community operation optimization / Lorenti, G., Lazzeroni, P., Repetto, M.. - (2025), pp. 884-891. (2025 International Conference on Clean Electrical Power (ICCEP)) [10.1109/iccep65222.2025.11143680].

Availability:
This version is available at: 11583/3003547 since: 2025-10-01T10:32:28Z

Publisher:
IEEE

Published
DOI:10.1109/iccep65222.2025.11143680

Terms of use:

This article is made available under terms and conditions as specified in the corresponding bibliographic description in the repository

Publisher copyright
IEEE postprint/Author's Accepted Manuscript

©2025 IEEE. Personal use of this material is permitted. Permission from IEEE must be obtained for all other uses, in any current or future media, including reprinting/republishing this material for advertising or promotional purposes, creating new collecting works, for resale or lists, or reuse of any copyrighted component of this work in other works.

(Article begins on next page)

19 November 2026

Detailed versus aggregated modeling in energy community operation optimization

Gianmarco Lorenti, Paolo Lazzeroni, Maurizio Repetto
Dipartimento Energia "Galileo Ferraris"
Politecnico di Torino
Turin, Italy
gianmarco.lorenti@polito.it, paolo.lazzeroni@polito.it, maurizio.repetto@polito.it

***Abstract*—Energy communities are key paradigms in the transition toward decentralized and renewable-based energy systems. However, their inherent complexity often makes their optimal operation computationally demanding. This paper compares two alternative formulations for the optimal operation of a renewable energy community composed of residential multifamily buildings with rooftop photovoltaics and battery storage. On one hand, a detailed model represents each building as an individual active node, while on the other a simplified formulation aggregates all active components into a single equivalent node. Both are formulated as Linear Programming problems and applied to a case study using one-year real household and building load data from northern Italy, with synthetic photovoltaic generation based on typical meteorological year data. Multiple sizing scenarios are tested. Results show that the simplified model closely matches the detailed one, with annual energy quantities and optimal costs differing by less than 0.2%. Instead, solution times are reduced by over 80%, confirming that careful aggregation can be a valid strategy when detailed node-level outputs are not required.**

***Index Terms*—energy communities, optimization, model reduction, linear programming.**

I. Introduction

The transition to decentralized and renewable-based energy systems has increased interest in local energy communities, among which Renewable Energy Communities (RECs) represent a promising framework for collective self-consumption, particularly at the residential scale [1]. RECs introduce a new paradigm where local producers, prosumers, and end users jointly manage distributed energy resources to increase self-sufficiency [2]. A defining feature is energy sharing via the public distribution grid, enabling the local use of self-produced renewable energy beyond traditional behind-the-meter consumption [3].

Modeling and optimization are essential for the design and operation of RECs, which can become complex even at a small scale. Linear Programming (LP) and Mixed-Integer Linear Programming (MILP) are commonly adopted for this purpose due to their balance between modeling detail and computational effort [4], [5]. While LP- and MILP-based approaches are well established in the multi-energy systems literature [6]–[8], their application to RECs is more recent. Early studies relied on single-node models with aggregated profiles [2], whereas more recent works have introduced multi-node formulations [9]–[11], enabling a finer representation of energy exchanges and of distributed technologies.

Multi-node models are especially relevant when generation, storage, and demand resources are distributed among participants [12]. In such cases, detailed formulations are required to capture physical self-consumption and virtual exchanges. However, increasing model detail also increases dimensionality and solution time, especially with longer time horizons and multiple technologies [11], [13], [14]. This creates a trade-off between model accuracy and computational efficiency, motivating research into model simplifications.

One possible simplification is aggregating multiple active nodes into a single equivalent unit. An improper aggregation can lead to misleading results, particularly when internal heterogeneity leads to virtual exchanges among nodes that would be lost in the aggregated representation. The effects of such simplification depends on the topology of the community, the allocation of technologies, and the variability of consumption and generation profiles.

Therefore, this work explores a case-specific simplification strategy for RECs composed of residential multifamily buildings. In this setup, households are considered passive participants, while buildings act as active nodes, with rooftop photovoltaic generators (PV), battery energy storage systems (BESS), and loads for common services. We compare a detailed model, where each building is an individual node, with a simplified model that aggregates all active components into a single equivalent node.

Both formulations are expressed as LP problems and applied to a case study based on real load data from a residential area near Turin (Italy), with PV generation modeled using typical meteorological year (TMY) data. A range of PV and BESS sizing scenarios is considered to compare model accuracy and computational effort.

The paper is organized as follows. Section II introduces the REC configuration under study. Section III describes the modeling framework and optimization problem. Section IV details the input data and simulation scenarios. Section V presents the numerical results and discusses the comparison between detailed and aggregated models. Finally, Section VI summarizes the main findings and outlines future research directions.

II. Energy Community of Residential Buildings

Fig. 1 shows the layout of an energy community composed of multiple residential buildings, in line with the Italian regulation RECs. These allow energy sharing among producers, prosumers, and consumers connected to the same low- or medium-voltage public distribution grid, without requiring private infrastructure.

Energy exchanges among users are "virtual", computed from *hourly* injection and withdrawal metered at each point of delivery:

$$E_{\mathrm{h}}^{\mathrm{shared}} := \min\left(\sum_{\mathrm{j}} E_{\mathrm{j,h}}^{\mathrm{inj}}, \sum_{\mathrm{j}} E_{\mathrm{j,h}}^{\mathrm{with}}\right), \tag{1}$$

where $E_{\mathrm{j,h}}^{\mathrm{inj}}$ and $E_{\mathrm{j,h}}^{\mathrm{with}}$ are the energy injected and withdrawn by user j at time step h.

Each building hosts PV on its rooftop to supply electricity to common services (e.g., elevators, lighting). This represents a form of physical self-consumption, as it occurs behind the meter and is directly measurable. Surplus generation is injected into the grid.

All households are connected to the public distribution grid and participate in energy sharing as defined in (1).

Withdrawals are paid at the retail price, injections are compensated at market value, and shared energy is incentivized through a fixed reward, typically lower than the retail–market price gap. This reflects the fact that, unlike physical self-consumption, shared energy uses the public grid and is subject to system charges and, partially, to distribution fees.

Nonetheless, participants are encouraged to coordinate generation and consumption to maximize both shared energy and self-consumption, improving renewable integration and reducing the dependence on centralized generation. To add flexibility, storage systems are considered. As shown in Fig. 1, BESS is installed alongside each PV plant and primarily supports self-consumption but can also be operated to increase shared energy within the community.

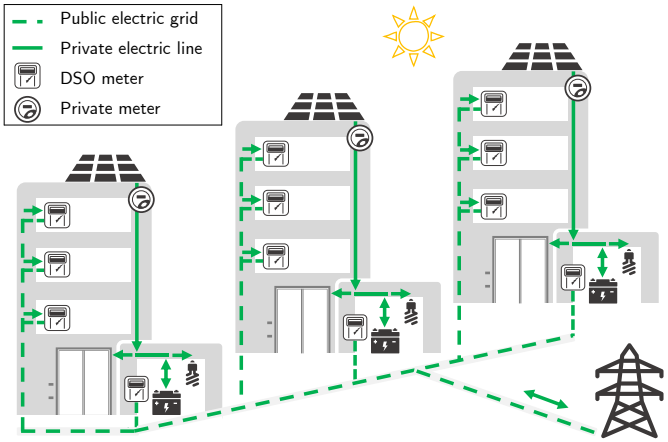


Fig. 1. Schematic layout of an energy community composed of residential buildings.

III. Modeling and Optimization

The energy community is modeled as a set of energy nodes interconnected through the distribution grid. Each residential building is an active node equipped with PV generation and BESS, supplying loads for common services. All household consumers are represented by a single passive node with an aggregated electric load.

The resulting model, shown in Fig. 2a, consists of a set of active nodes $\mathcal{J} = \{1, \ldots, J\}$ and one passive node. This model distinguishes between within-node balances (physical self-consumption) and inter-node exchanges (virtual energy sharing). The main model variables are listed in Table I, with subscript j indicating building-specific quantities.

To reduce dimensionality, a simplified model is introduced (Fig. 2b), which aggregates all active components into a single equivalent node $\mathcal{J}' = \{\mathrm{tot}\}$, while the passive node remains unchanged. Aggregated quantities are defined as:

$$\begin{aligned} P_{\mathrm{aggr}}^{\mathrm{UE}} &= \sum_{\mathrm{j}} P_{\mathrm{j}}^{\mathrm{UE}}, \\ S_{\mathrm{tot}}^{\mathrm{PV}} = \sum_{\mathrm{j}} S_{\mathrm{j}}^{\mathrm{PV}}, &\qquad S_{\mathrm{tot}}^{\mathrm{BESS}} = \sum_{\mathrm{j}} S_{\mathrm{j}}^{\mathrm{BESS}}, \end{aligned} \tag{2}$$

where S^{PV} and S^{BESS} denote PV and BESS capacities, in kW and kW h, respectively.

An LP formulation is adopted to optimize community operation over a defined time horizon. The following equations define the constraints and the objective function of the problem. All constraints apply to each $j \in \mathcal{J}$ (or $\mathcal{J}'$) and $h \in \mathcal{H}$, though index ranges are omitted for brevity.

The power balance at each active node reads as follows:

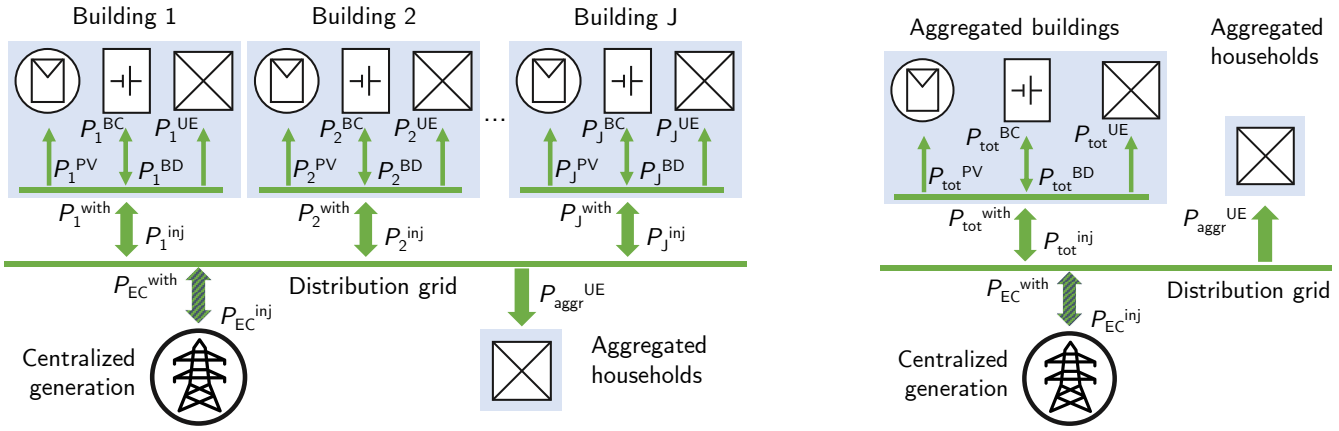
$$P_{\mathrm{j,h}}^{\mathrm{PV}} + P_{\mathrm{j,h}}^{\mathrm{BD}} + P_{\mathrm{j,h}}^{\mathrm{with}} = P_{\mathrm{j,h}}^{\mathrm{UE}} + P_{\mathrm{j,h}}^{\mathrm{BC}} + P_{\mathrm{j,h}}^{\mathrm{inj}}. \tag{3}$$

BESS is modeled with a time-coupled balance:

$$E_{\mathrm{j,k}}^{\mathrm{stor}} = \eta_{\mathrm{sd}} E_{\mathrm{j,h}}^{\mathrm{stor}} + \left(\eta_{\mathrm{c}} P_{\mathrm{j,h}}^{\mathrm{BC}} - \frac{P_{\mathrm{j,h}}^{\mathrm{BD}}}{\eta_{\mathrm{d}}}\right) \Delta t_{\mathrm{h}}, \tag{4}$$

TABLE I
Main inputs and variables of the LP optimization problem.

	Symbol	Description	Unit
Inputs	$P_{\mathrm{j,h}}^{\mathrm{PV}}$	Photovoltaic generation	kW
	$P_{\mathrm{j,h}}^{\mathrm{UE}}$	Electric load for common services	kW
	$P_{\mathrm{aggr,h}}^{\mathrm{UE}}$	Aggregated households electric load	kW
Variables	$P_{\mathrm{j,h}}^{\mathrm{inj}}$	Grid injection	kW
	$P_{\mathrm{j,h}}^{\mathrm{with}}$	Grid withdrawal	kW
	$P_{\mathrm{j,h}}^{\mathrm{BC}}$	Battery charge	kW
	$P_{\mathrm{j,h}}^{\mathrm{BD}}$	Battery discharge	kW
	$E_{\mathrm{j,h}}^{\mathrm{stor}}$	Energy currently stored in the battery	kW h
	$E_{\mathrm{h}}^{\mathrm{shared}}$	Shared energy	kW h



(a) Detailed model

(b) Simplified model

Fig. 2. Schematic representation of the energy community, with power balances: multi-node versus aggregated modeling.

where $k = h+1$ except for the last time step, for which $k = 0$, enforcing periodicity. The parameters η_{sd}, η_{c}, and η_{d} represent self-discharge, charge, and discharge efficiencies, respectively.

Operational constraints include power and energy limits:

$$\begin{aligned} \mathrm{SOC}_{\min} S_{\mathrm{j}}^{\mathrm{BESS}} \le E_{\mathrm{j,h}}^{\mathrm{stor}} \le \mathrm{SOC}_{\max} S_{\mathrm{j}}^{\mathrm{BESS}}, \\ P_{\mathrm{j,h}}^{\mathrm{BC}} \le S_{\mathrm{j}}^{\mathrm{BESS}}/t_{\mathrm{c,min}}, \qquad P_{\mathrm{j,h}}^{\mathrm{BD}} \le S_{\mathrm{j}}^{\mathrm{BESS}}/t_{\mathrm{d,min}}, \end{aligned} \tag{5}$$

with $t_{\mathrm{c,min}}$ and $t_{\mathrm{d,min}}$ being the minimum charge and discharge times (in hours); $\mathrm{SOC}_{\min}$ and $\mathrm{SOC}_{\max}$ being the minimum and maximum state of charge values.

The shared energy expression in (1) involves a minimum function, which is linearized through the following constraints:

$$\begin{aligned} E_{\mathrm{h}}^{\mathrm{shared}} &\le \sum_{\mathrm{j}} P_{\mathrm{j,h}}^{\mathrm{inj}} \Delta t_{\mathrm{h}}, \\ E_{\mathrm{h}}^{\mathrm{shared}} &\le \left(\sum_{\mathrm{j}} P_{\mathrm{j,h}}^{\mathrm{with}} + P_{\mathrm{aggr,h}}^{\mathrm{UE}} \right) \Delta t_{\mathrm{h}}. \end{aligned} \tag{6}$$

Since E^{shared} is maximized in the objective function in (7), the solver will push it to the minimum of the two upper bounds, enforcing the original definition.

The objective function minimizes total system costs over time:

$$\begin{aligned} \text{minimize} \sum_{\mathrm{h}} \Bigg[\left(\sum_{\mathrm{j}} P_{\mathrm{j,h}}^{\mathrm{with}} + P_{\mathrm{aggr,h}}^{\mathrm{UE}} \right) \Delta t_{\mathrm{h}} c_{\mathrm{h}}^{\mathrm{with}} \\ - \sum_{\mathrm{j}} P_{\mathrm{j,h}}^{\mathrm{inj}} \Delta t_{\mathrm{h}} c_{\mathrm{h}}^{\mathrm{inj}} - E_{\mathrm{h}}^{\mathrm{shared}} c_{\mathrm{h}}^{\mathrm{shared}} \Bigg], \end{aligned} \tag{7}$$

where c^{with}, c^{inj}, and c^{shared} are the retail, market, and REC incentive rates. Note that $P_{\mathrm{aggr,h}}^{\mathrm{UE}}$ is not a decision variable but is included to reflect the community's total energy cost.

The LP structure remains identical for both configurations; the only difference is the set of active nodes: $\mathcal{J}$ in the detailed case and $\mathcal{J}'$ in the simplified one. This significantly affects problem size, as summarized in Table II, where H is the number of time steps.

TABLE II
PROBLEM SIZE DEPENDING ON THE MODEL.

	Detailed model	Simplified model
Variables	$6JH + H$	$7H$
Equality constraints	$2JH$	$2H$
Inequality constraints	$3JH + 2H$	$5H$

IV. Case Study

The detailed and simplified models in Fig. 2 are tested and compared using one year of hourly electricity demand data (March 2021 – March 2022), measured in a small city near Turin, northern Italy. The dataset includes 10 residential buildings, used directly for an equal number active nodes, and 30 households, which are aggregated and scaled to represent 300 users –i.e., 30 per building. Annual energy consumption is 13.5 MW h for buildings and 771 MW h for households (i.e., 2.57 MW h per household).

Hourly PV generation is synthetically generated from PVGIS typical meteorological year data for the same location. To introduce variability across profiles, tilt and azimuth angles are combined from $\{-90°, -45°, 0°, +45°, +90°\}$ and $\{20°, 30°\}$, and randomly assigned to the buildings. The resulting annual PV yield ranges from 1209 to 1574 kWh/kW, with an average of 1387 kWh/kW.

Fig. 3 shows the monthly energy values obtained from these profiles, considering aggregated values, while Fig. 4 focuses on a single representative day. The figure illustrates both the aggregated profile and the building-level detail, highlighting differences in both consumption and production among buildings, with the latter influenced by varying tilt and azimuth angles of the PV systems. Six PV–BESS combinations are tested for a robust comparison of the two optimization models, as summarized in Table III. Two PV capacities are considered: 60 kW per building (600 kW total), which matches the REC's annual demand, and an increased 90 kW per building (900 kW total). These values do not account for rooftop availability

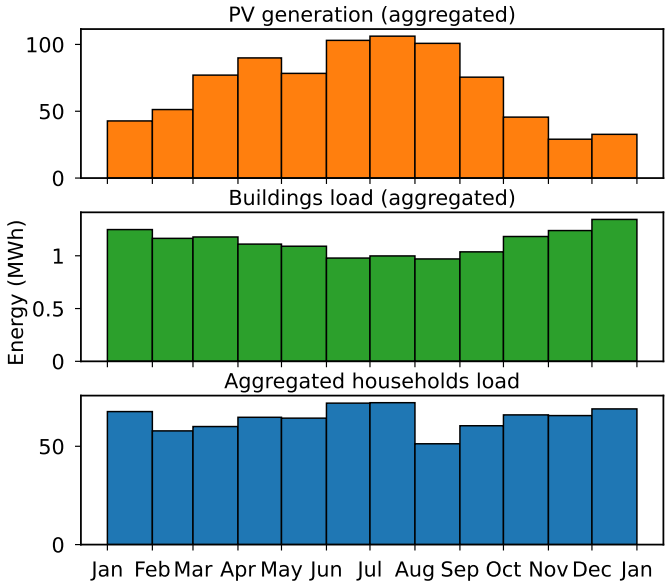


Fig. 3. Monthly aggregated energy: PV generation, building loads, and household loads.

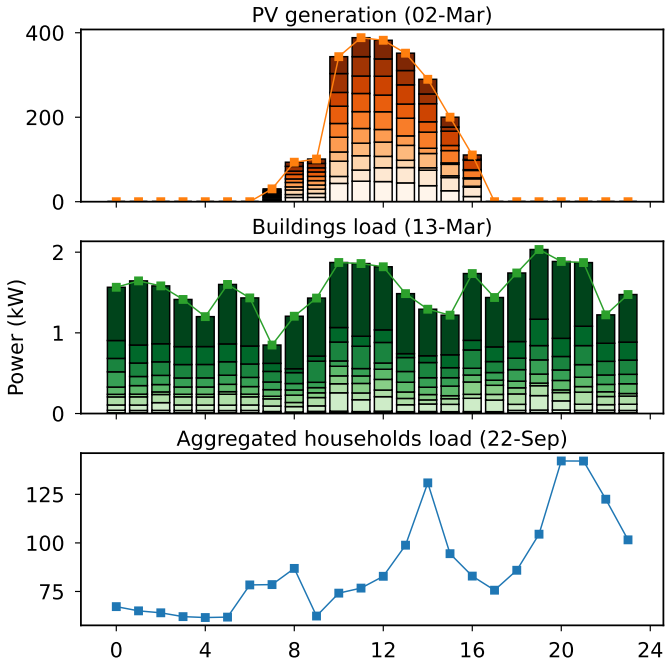


Fig. 4. PV generation, building loads, and household load profiles on a representative day, selected as the one with daily energy closest to the yearly median. The solid line with markers represents aggregated values, while the stacked bars show the building-level detail.

constraints —an aspect relevant in a sizing study— as it is meant to provide a set of scenarios for comparing operational outcomes under predefined configurations.

In all cases, component sizes are equally distributed across buildings: $S_{\mathrm{j}}^{\mathrm{PV}} = S_{\mathrm{tot}}^{\mathrm{PV}}/10$, $S_{\mathrm{j}}^{\mathrm{BESS}} = S_{\mathrm{tot}}^{\mathrm{BESS}}/10$.

Electricity prices and incentives are based on 2024 data from the Italian market and are assumed constant (see Table IV).

TABLE III
TESTED COMBINATIONS OF PV AND BESS SIZES.

		1	2	3	4	5	6
$S_{\mathrm{tot}}^{\mathrm{PV}}$	(kW)	600	600	600	900	900	900
$S_{\mathrm{tot}}^{\mathrm{BESS}}$	(kW h)	0	600	1200	0	900	1800

TABLE IV
ELECTRICITY PRICES (2024 AVERAGES).

Parameter	Description	Value (€/kWh)
c^{with}	Grid withdrawal (retail price)	0.313
c^{inj}	Grid injection (market value)	0.109
c^{shared}	Shared energy incentive	0.142

BESS parameters are set as: $\eta_{\mathrm{sd}} = 0.995$, $\eta_{\mathrm{c}} = 0.98$, $\eta_{\mathrm{d}} = 0.94$, $t_{\mathrm{c,min}} = t_{\mathrm{d,min}} = 2\,\mathrm{h}$, $\mathrm{SOC}_{\mathrm{min}} = 0$, $\mathrm{SOC}_{\mathrm{max}} = 0.8$.

The LP model is solved over the full-year horizon for both detailed and simplified models using Python and GUROBI. The comparison focuses on:

- optimal objective values,
- key decision variables (e.g., BESS operation),
- computational complexity.

V. RESULTS AND DISCUSSION

Table V compares the optimization results for all six PV and BESS configurations using the detailed and aggregated models. For each case, it reports the optimal objective value, the time to solve the LP, and the annual energy quantities obtained by summing hourly values of key variables: BESS operation (E^{BC}, E^{BD}), grid exchanges (E^{inj}, E^{with}), and shared energy (E^{shared}). Each configuration includes a Δ row, showing the relative percentage difference between the aggregated and detailed models, using the latter as the reference –i.e., the "correct" solution.

These results show that the aggregated model yields virtually identical outcomes, with differences below 0.2% across all metrics. Interestingly, small differences in the shared energy value also arise in the configurations without BESS, where no optimization is performed and only energy balances are enforced: aggregation reduces the mismatch between individual consumption and generation profiles, leading to an artificial increase in physical self-consumption.

The only notable difference remains computational, with the aggregated model consistently reducing solution time by more than 80%, and up to nearly 90% in high-dimensional cases.

To investigate differences in optimization variables at the level of the individual time steps, a more detailed comparison is carried out for the configuration with $S_{\mathrm{tot}}^{\mathrm{PV}} = 900\,\mathrm{kW}$ and $S_{\mathrm{tot}}^{\mathrm{BESS}} = 1800\,\mathrm{kW\,h}$, exhibiting the highest deviation in the optimal objective.

Fig. 5 shows the BESS charge and grid injection profiles on the day with the highest absolute deviation between models. A significant difference appears only at specific time steps during BESS charging, while the overall daily behavior remains

TABLE V
COMPARISON OF THE OPTIMIZATION RESULTS BETWEEN THE DETAILED MODEL WITH 10 ACTIVE NODES AND THE AGGREGATED ONE, FOR DIFFERENT PV AND BESS SIZES.

Configuration $S^{\text{PV}}_{\text{tot}}$ (kW)	Configuration $S^{\text{BESS}}_{\text{tot}}$ (kWh)	Model	Optimal objective (€$\times 10^3$)	Time to solve (s)	E^{BC} (MWh)	E^{BD} (MWh)	E^{inj} (MWh)	E^{with} (MWh)	E^{shared} (MWh)
600	0	Detailed	111.49	14.23	–	–	527.87	480.18	298.24
		Aggregated	111.49	2.81	–	–	527.87	480.18	298.20
		Δ(%)	**0.00**	**-80.25**	–	–	**0.00**	**0.00**	**-0.01**
600	600	Detailed	94.72	50.08	153.26	132.62	376.22	349.17	421.85
		Aggregated	94.72	6.34	153.26	132.65	376.24	349.17	421.81
		Δ(%)	**-0.01**	**-87.35**	**0.00**	**0.02**	**0.01**	**0.00**	**-0.01**
600	1200	Detailed	82.02	58.09	280.30	238.72	249.45	243.34	527.71
		Aggregated	82.01	6.57	280.32	238.75	249.46	243.34	527.64
		Δ(%)	**-0.01**	**-88.69**	**0.01**	**0.02**	**0.01**	**0.00**	**-0.01**
900	0	Detailed	63.69	15.55	–	–	925.65	461.85	316.54
		Aggregated	63.69	2.82	–	–	925.65	461.85	316.51
		Δ(%)	**0.00**	**-81.84**	–	–	**0.00**	**0.00**	**-0.01**
900	900	Detailed	37.93	52.29	236.82	204.53	689.89	258.38	512.60
		Aggregated	37.92	6.03	236.77	204.55	689.96	258.38	512.60
		Δ(%)	**-0.02**	**-88.47**	**-0.02**	**0.01**	**0.01**	**0.00**	**0.00**
900	1800	Detailed	22.71	56.08	396.54	334.93	530.39	128.20	643.15
		Aggregated	22.68	6.06	396.49	334.92	530.43	128.20	642.77
		Δ(%)	**-0.12**	**-89.20**	**-0.01**	**0.00**	**0.01**	**0.00**	**-0.06**

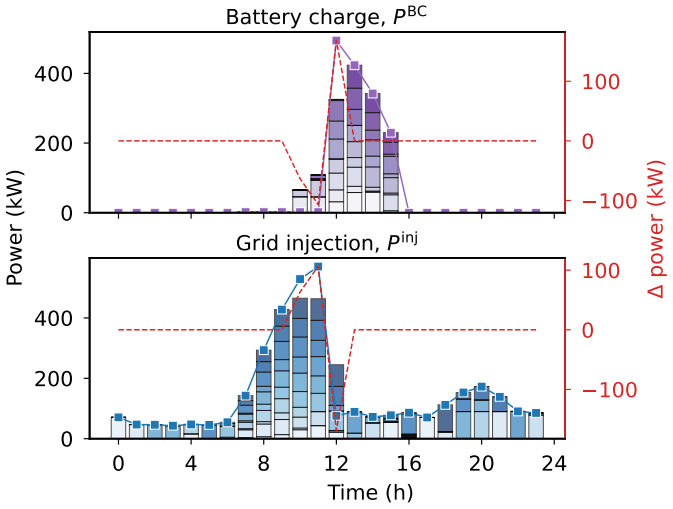


Fig. 5. Battery charge and grid injection profiles for the day with the maximum deviation between the detailed and aggregated models. The solid line represents the aggregated model, while the colored bars represent the contribution of individual buildings in the detailed model, each color corresponding to a different building. The right y-axis shows the difference between the detailed model (sum of the bars) and the aggregated one.

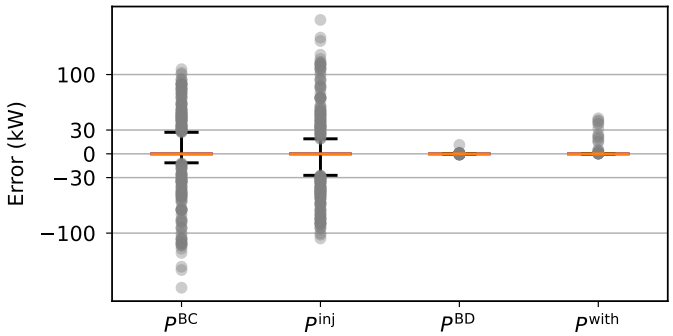


Fig. 6. Boxplot of the time step-by-time step error between aggregated and detailed model outputs for the main optimization variables. For the detailed model, the sum over all active nodes is considered. Whiskers correspond to the 1st and 99th percentiles, while outliers are marked as dots.

consistent. In this case, the aggregated model delays storage, swapping the time steps in which excess energy is stored or injected into the grid (due to storage being full), but the resulting daily energy balance is practically unchanged.

The comparison is extended over the full year in Fig. 6 and Fig. 7, which show boxplots of the errors for four key optimization variables. In both cases, the output of the aggregated model is compared against the sum of the corresponding values from the detailed model. Fig. 6 reports the time step-by-time step error. Whiskers are set to the 1st and 99th percentiles, and time steps beyond these thresholds are plotted as outliers (dots). Hence, more than 98% of the time steps show an error below 30 kW for all variables. The boxes, defined by the 25th and 75th percentiles, are not visible, indicating that the error remains extremely close to zero for most time steps.

Fig. 7 presents the same comparison in percentage terms, computed against the corresponding value in the detailed model. The number of time steps within a ±1% deviation is shown on the bottom-right corner of the figure. While a few extreme values reach up to 100%, these are limited to rare cases, such as the one shown in Fig. 5, where energy flows are temporally shifted between storage and grid injection.

Table VI provides a quantitative summary of the percentage time-step errors across all configurations, extending the

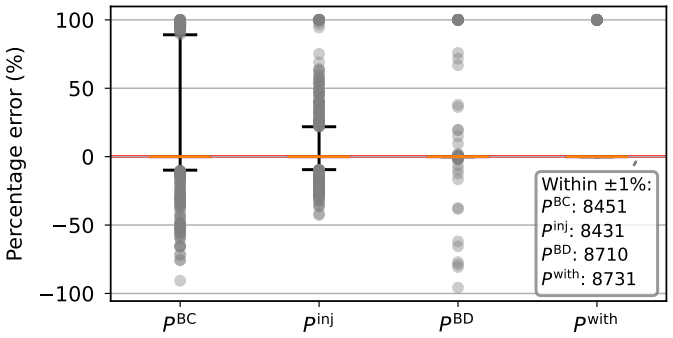


Fig. 7. Boxplot of the percentage error between aggregated and detailed model outputs. An annotation indicates the time steps falling within a $\pm 1\%$ band, highlighted as a shaded area.

analysis in Fig. 7. It reports mean and key-percentiles error values, and the number of time steps falling within 1% and 10% deviation from the detailed model (out of 8760 total).

Table VII further explains the close agreement observed between the aggregated and detailed model outputs. It reports the number of time steps in which at least one building injects into the grid while another simultaneously withdraws. These are the time steps when virtual exchanges among buildings may occur and could, therefore, be lost in the aggregated formulation. As shown, such time steps are less than 1% of the total when BESS is included. This confirms that inter-building interactions are rare under the considered conditions, which helps explain the minimal error observed across all configurations.

When no BESS is present, this condition is evaluated based only on the PV generation and building loads, providing insight into the alignment between generation and consumption profiles across buildings. Therefore, this outcome may not be generalized to energy communities with more heterogeneous active nodes, where greater diversity in generation or load could increase the potential for inter-building exchanges and reduce the accuracy of aggregated models.

VI. Conclusion and Perspectives

This paper compared two formulations for the optimal operation of a renewable energy community composed of residential multifamily buildings. In the considered setup, buildings equipped with rooftop photovoltaics and battery storage act as active nodes, supplying electricity to common loads (physical self-consumption) and injecting surplus energy into the grid for virtual exchange with households and among buildings. The detailed model treats each building as an individual node, while the simplified model aggregates all active components into a single equivalent node. Both configurations were formulated as LP problems and applied to a case study based on real load data from a city near Turin, with PV generation simulated from typical meteorological year data.

TABLE VI
Statistical summary of time-step percentage errors between aggregated and detailed models across all PV and BESS configurations for the main power variables.

Configuration S^{PV}_{tot} (kW)	Configuration S^{BESS}_{tot} (kWh)	Variable	1st percentile (%)	Mean (%)	Median (%)	99th percentile (%)	Within ±1% (time steps)	Within ±10% (time steps)
600	0	P^{BC}	–	–	–	–	–	–
		P^{inj}	0.00	0.85	0.00	18.22	8600	8651
		P^{BD}	–	–	–	–	–	–
		P^{with}	0.00	1.53	0.00	100.00	8593	8608
600	600	P^{BC}	-25.47	2.58	0.00	97.28	8140	8248
		P^{inj}	-9.96	1.06	0.00	43.54	8101	8450
		P^{BD}	-0.05	0.66	0.00	5.28	8627	8657
		P^{with}	0.00	0.30	0.00	0.00	8734	8734
600	1200	P^{BC}	-13.54	1.42	0.00	91.19	8372	8442
		P^{inj}	-8.59	0.90	0.00	34.90	8311	8528
		P^{BD}	-0.17	0.53	0.00	4.25	8616	8648
		P^{with}	0.00	0.47	0.00	0.00	8719	8719
900	0	P^{BC}	–	–	–	–	–	–
		P^{inj}	0.00	0.61	0.00	5.85	8647	8682
		P^{BD}	–	–	–	–	–	–
		P^{with}	0.00	1.14	0.00	100.00	8634	8645
900	900	P^{BC}	-35.56	2.96	0.00	98.44	8096	8188
		P^{inj}	-13.06	0.78	0.00	40.79	8063	8393
		P^{BD}	0.00	0.57	0.00	0.00	8662	8682
		P^{with}	0.00	0.10	0.00	0.00	8751	8751
900	1800	P^{BC}	-10.01	1.12	0.00	89.22	8451	8498
		P^{inj}	-9.50	0.37	0.00	21.89	8431	8550
		P^{BD}	0.00	0.21	0.00	0.00	8710	8721
		P^{with}	0.00	0.33	0.00	0.00	8731	8731

TABLE VII
NUMBER OF TIME STEPS IN WHICH AT LEAST ONE BUILDING INJECTS AND ANOTHER WITHDRAWS ENERGY SIMULTANEOUSLY.

Configuration		Time steps
$S_{\text{tot}}^{\text{PV}}$ (kW)	$S_{\text{tot}}^{\text{BESS}}$ (kWh)	
	0	174
600	600	4
	1200	9
	0	127
900	900	4
	1800	20

Six PV and BESS sizing scenarios were considered to compare model outputs in terms of accuracy and computational effort.

The results demonstrated a strong agreement between the aggregated and detailed models across all tested configurations. Differences in annual energy quantities and optimal objective values were consistently below 0.2%. Solution times, on the other hand, were reduced by more than 80%, reaching almost 90% in the most complex scenarios.

A time step-by-time step analysis of the individual optimization variables over the considered time horizon further revealed that the vast majority of values fall within narrow error bands, with over 90% of time steps showing deviations below 1% in all cases. Deviations were observed in battery operation, with minor anticipations or delays in charging and discharging cycles, without affecting overall balances.

Further analysis revealed that the limited error is due to the few occurrences of simultaneous injection and withdrawal across different buildings –a condition under which aggregation may cause information loss. In the considered cases, these time steps account for less than 1% of the year, justifying the negligible discrepancy.

However, energy communities with more heterogeneous nodes (e.g., mixing residential, commercial, or industrial users) or installed technologies may exhibit more frequent inter-node exchanges, potentially reducing the reliability of the simplified formulation. In such cases, active nodes could be aggregated based on technological configurations or similarities between production and consumption profiles, creating multiple aggregated active nodes.

Moreover, despite the close match between the two formulations, the model does not account for technology-specific phenomena such as battery degradation, which may evolve differently when storage is aggregated versus distributed across buildings. Including degradation effects would be particularly relevant in long-term planning.

Finally, the present analysis compares aggregated quantities from the detailed model to those from the simplified one. This is valid when the goal is to assess system-level operation or the global sizing of technologies. However, in scenarios where node-level information is required, a disaggregation step would be necessary, e.g., to allocate costs and benefits or to use the model as part of a sizing procedure for individual components. In those cases, a disaggregation strategy should be defined, and its impact should be evaluated at the individual node level, which goes beyond the scope of this study and remains a topic for future investigation.

Apart from addressing the above limitations, future work will focus on comparing the two formulations in setups involving multiple energy carriers, where interactions between different systems may lead to greater discrepancies between aggregated and detailed representations. The framework will also be integrated into a broader design optimization loop to assess how the choice of model influences sizing outcomes. Finally, it will be important to explore how uncertainty in input data (e.g., load profiles, weather conditions) affects the results, particularly with respect to how uncertainty is quantified in aggregated versus disaggregated models.

REFERENCES

[1] A. Canova, P. Lazzeroni, G. Lorenti, F. Moraglio, A. Porcelli, and M. Repetto, "Decarbonizing residential energy consumption under the Italian collective self-consumption regulation," *Sustainable Cities and Society*, vol. 87, p. 104196, 2022. doi:10.1016/j.scs.2022.104196.

[2] A. Cielo, P. Lazzeroni, P. Margiaria, I. Mariuzzo, and M. Repetto, "Renewable Energy Communities business models under the 2020 Italian regulation," *Journal of Cleaner Production*, vol. 316, p. 128217, 2021. doi:10.1016/j.jclepro.2021.128217.

[3] V. Z. Gjorgievski, S. Cundeva, and G. E. Georghiou, "Social arrangements, technical designs and impacts of energy communities: A review," *Renewable Energy*, vol. 169, pp. 1138–1156, 2021.

[4] S. Rech, "Smart Energy Systems: Guidelines for Modelling and Optimizing a Fleet of Units of Different Configurations," *Energies*, vol. 12, no. 7, p. 1320, 2019. doi:10.3390/en12071320.

[5] G. Chicco and A. Mazza, "Metaheuristic optimization of power and energy systems: Underlying principles and main issues of the 'rush to heuristics'," *Energies*, vol. 13, no. 19, 2020. doi:10.3390/en13195097.

[6] C. Klemm and P. Vennemann, "Modeling and optimization of multi-energy systems in mixed-use districts: A review of existing methods and approaches," *Renewable and Sustainable Energy Reviews*, vol. 135, p. 110206, 2021. doi:10.1016/j.rser.2020.110206.

[7] E. Widl, D. Cronbach, P. Sorknæs, J. Fitó, D. Muschick, M. Repetto, J. Ramousse, and A. Ianakiev, "Expert survey and classification of tools for modeling and simulating hybrid energy networks," *Sustainable Energy, Grids and Networks*, vol. 32, 2022. 10.1016/j.segan.2022.100913.

[8] M. Fodstad, P. Crespo del Granado, L. Hellemo, B. R. Knudsen, P. Pisciella, A. Silvast, C. Bordin, S. Schmidt, and J. Straus, "Next frontiers in energy system modelling: A review on challenges and the state of the art," *Renewable and Sustainable Energy Reviews*, vol. 160, p. 112246, 2022. doi:10.1016/j.rser.2022.112246.

[9] G. Coletta and L. Pellegrino, "Optimal Design of Energy Communities in the Italian Regulatory Framework," in *2021 AEIT International Annual Conference (AEIT)*, pp. 1–6, 2021. doi:10.23919/AEIT53387.2021.9626852.

[10] A. Cosic, M. Stadler, M. Mansoor, and M. Zellinger, "Mixed-integer linear programming based optimization strategies for renewable energy communities," *Energy*, vol. 237, p. 121559, 2021. doi:10.1016/j.energy.2021.121559.

[11] E. Dal Cin, G. Carraro, G. Volpato, A. Lazzaretto, and P. Danieli, "A multi-criteria approach to optimize the design-operation of Energy Communities considering economic-environmental objectives and demand side management," *Energy Conversion and Management*, vol. 263, p. 115677, 2022. doi:10.1016/j.enconman.2022.115677.

[12] P. Lazzeroni, G. Lorenti, F. Moraglio, and M. Repetto, "Modeling of Renewable Energy Communities: the RECoupled approach," in *2022 IEEE 46th Annual Computers, Software, and Applications Conference (COMPSAC)*, pp. 1349–1354, 2022. doi:10.1109/COMPSAC54236.2022.00213.

[13] I. Mariuzzo, D. Fioriti, E. Guerrazzi, D. Thomopulos, and M. Raugi, "Multi-objective planning method for renewable energy communities with economic, environmental and social goals," *International Journal of Electrical Power & Energy Systems*, vol. 153, p. 109331, 2023. doi:10.1016/j.ijepes.2023.109331.

[14] R. J. De Souza, M. Reini, L. M. Serra, M. A. Lozano, E. Nadalon, and M. Casisi, "Multi-Objective Optimization of an Energy Community Powered by a Distributed Polygeneration System," *Energies*, vol. 17, no. 13, 2024. 10.3390/en17133085.